Chapter 3

Application of the Bayesian Approach to Incorporate Helium Isotope Ratios in Long-Term Probabilistic Volcanic Hazard Assessments in Tohoku, Japan

Andrew James Martin, Koji Umeda and Tsuneari Ishimaru

Additional information is available at the end of the chapter

http://dx.doi.org/10.5772/51859

1. Introduction

Geological hazard assessments based on established statistical techniques are now commonly used as a basis to make decisions that may affect society over the long-term (0.1 – 1 Ma). Volcanic risk essentially consists of:

(1) The probability of a 'volcanic event' occurring such as a dike intrusion or a new strato- or caldera volcano forming e.g. [1- 7]

(2) The consequences of the volcanic event e.g. [8 - 9].

A challenge with the long-term probabilistic assessment of future volcanism in relation to the siting of, for example geological repositories is that because new volcano formation is rare, uncertainties in models are inherently large [10]. Sites for nuclear facilities in particular must be located in areas of very low geologic risk [11]. Recent studies have been carried out looking at the hazard posed by volcanoes to nuclear power plants in Armenia [e.g. 9, 12] and Java, Indonesia [e.g. 13]. Here the focus was more on the consequences of an eruption at an existing volcano on the safety of an operating nuclear power plant. In the case of a geological repository for high and/or low level radioactive waste, the emphasis is on the consequences of new igneous activity such as a dike that may intrude the repository [e.g. 14] and transport the waste to the surface. In this case, the probability of a new volcano forming in the first place is very low (typically < 10^{-7}/a) since by definition such facilities should be located away from existing Quaternary volcanoes. However the lack of volcano 'data' implies that addition information on the processes that control future long-term spatio-temporal distribution of volcanism are

needed. This has motivated several investigators to incorporate datasets in addition to the distribution and timing of past volcanic activity in volcanic probabilistic analyses [e.g. 15]. Bayesian inference has been used to combine geophysical datasets to probability distributions constructed from known historic volcano locations in order to estimate the location of future volcanism over a regional scale [1]. More recently, [16] used Bayesian inference to merge prior information and past data to construct a probability map of vent opening at the Campi Flegrei caldera in Italy.

Here we revisit the Bayesian approach developed by [1] where seismic tomographs and geothermal gradients were incorporated into probabilistic assessments by Bayesian inference in Tohoku. We apply the same Bayesian technique in the same study area to incorporate recently acquired helium isotopes into probabilistic hazard assessments; such noble gases have been shown to be excellent natural tracers for mantle-crust interaction owing to their inert chemical properties which means they are not altered by complex chemical processes. Moreover helium isotopes provide evidence for the presence of mantle derived materials in the crust, owing to the distinct isotopic compositions between the crust and the upper mantle [e.g. 17, 18]. We examine the link between volcanism and $^{3}He/^{4}He$ ratios that may infer possible regions of magma generation and hence volcano formation. Such links between magmatism and elevated $^{3}He/^{4}He$ ratios have been proposed [e.g. 19, 20], but the link has not been examined quantitatively in probabilistic based models. Finally we discuss the Bayesian method in developed by [1] in the context of recent approaches to incorporate multiple datasets [e.g. 21, 22].

2. Japan and the Tohoku region

Japan is one of the most tectonically active regions in the world. Due to the dynamics of four plates, Quaternary volcanoes have formed along distinct volcanic fronts in east and west Japan (Figure 1).

The Tohoku region (Figure 2) is arguably one of the most extensively studied volcanic arcs in the world, particularly regarding the relationship between volcanism and tectonics. Moreover there have been numerous geological and geophysical investigations yielding high-quality datasets e.g., [23 - 29].

Tohoku is a mature double volcanic arc with a back-arc marginal sea basin located on a convergent plate boundary of the subducting Pacific plate and the North American plate (Figure 1). The location and orientation of the volcanic front (grey line in Figure 2) has been linked to the opening of the Sea of Japan and subduction angle of the Pacific plate [e.g., 26, 33]. From 60 Ma up until about 10 Ma the volcanic front migrated east and west several times, however, it has been relatively static during the last 8 Ma [26].

Presently there are 15 known historically active volcanoes in the Tohoku region and a total 170 volcanoes that formed during the Quaternary [30]. Volcanism has gradually become more clustered and localized over a period from 14 Ma to present [34], thus volcano clustering is a characteristic feature in Tohoku.

http://dx.doi.org/10.5772/51859

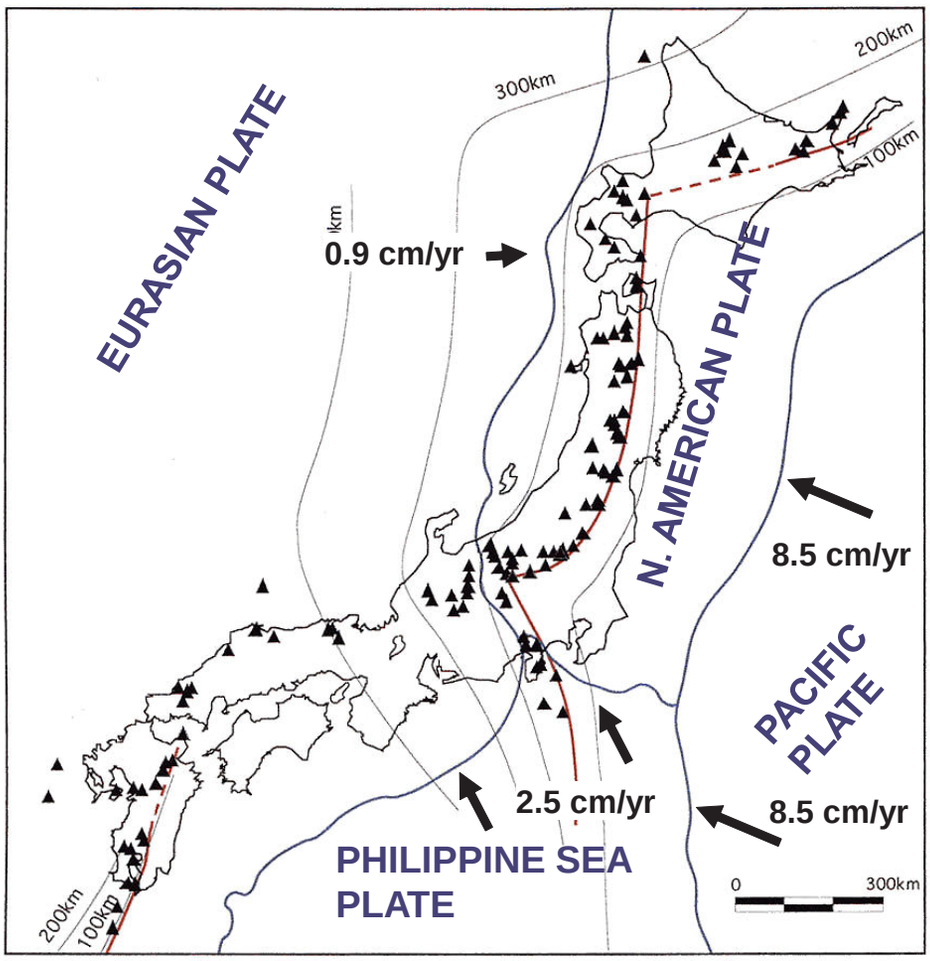

Figure 1. Map showing the tectonic setting of Japan (Figure modified from [1]). The four main islands that make up Japan are located on or near the boundaries of four plates. Black triangles denote Quaternary volcanoes and the red lines depict the main volcanic fronts. The thin contour lines denote the depth of the subducting Pacific Plate beneath Japan. The velocities and arrows indicate the subduction rates and directions respectively of the Pacific, Philippine Sea and Eurasian plates relative to the North American plate.

3. Defining the volcanic event

What do we mean here by 'volcano'? In developing probabilistic based models, one of the most difficult and challenging tasks is defining the 'volcanic event'. This is because the volcanic event defined has to be simple and consistent enough for the probabilistic based models to handle. To a certain extent the degree of consistency that can be realistically included in a model is largely constrained by the size of the study area and by the amount and quality of geological, geochemical and/or geophysical data available. The volcanic event could range from a single eruption to a series of eruptions. It could be defined as the existence of a relatively young cinder cone, spatter mound, maar, tuff ring, tuff cone, pyroclastic fall, lava flow or even a large composite volcano. On the other hand older edifices may have been eroded and/or covered by sedimentary deposits such as alluvium and thus be more difficult to locate and/or

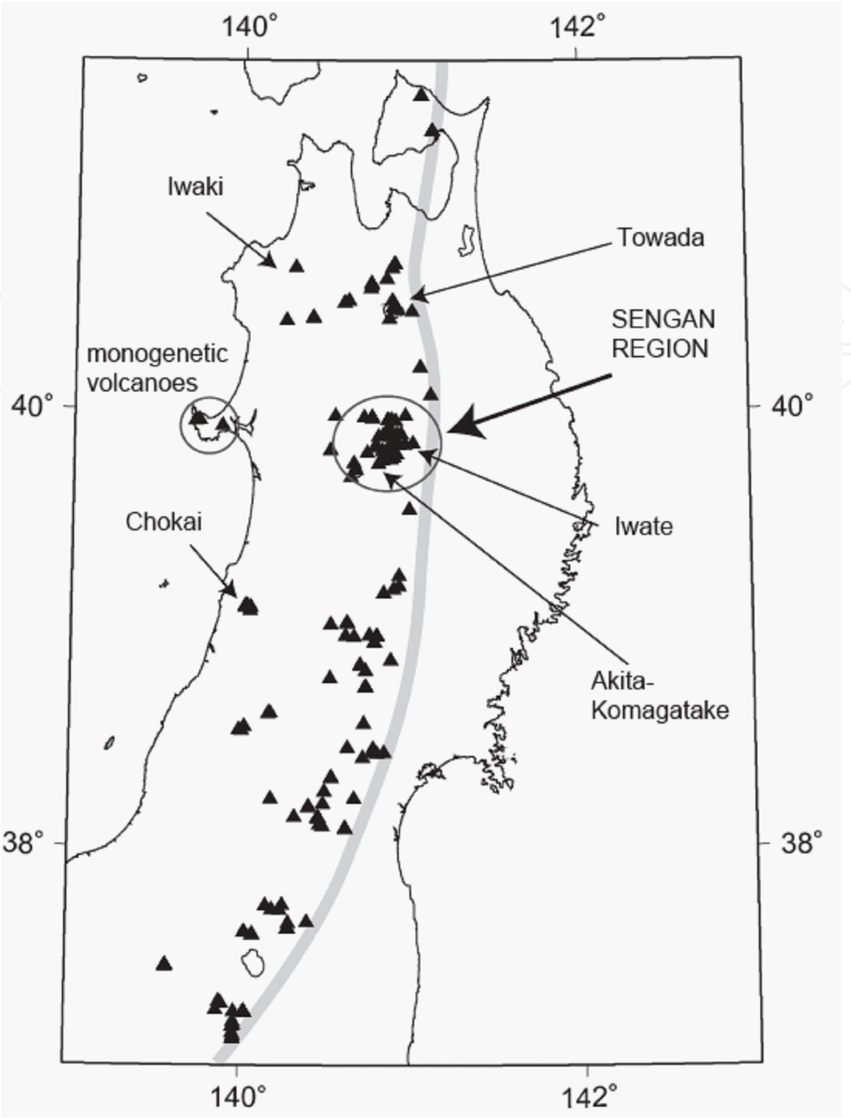

Figure 2. The volcanic arc in Tohoku consists of approximately 170 Quaternary edifices [28, 30] (modified from [1]). The highest density of volcanoes in Tohoku is the cluster in the Sengan region. Other notable volcanoes are the Towada volcano which has been the site of late Quaternary large-volume felsic eruptions resulting in large caldera formation [e.g., 27, 31], and the Iwaki and Chokai [32] volcanoes which are active andesitic volcanoes on the back-arc side of Tohoku. The grey line denotes the present day volcanic front.

are easily overlooked. Results of magnetic and gravity data have been used as evidence for locating such hidden volcanic events which in turn had an impact on resulting probabilities at given locations [e.g. 15].

If we were carrying out a hazard assessment on a single volcano we may be interested in defining the event as a series of pyroclastic flows or surges or eruptions that generate lava flows that exceed a certain volume [e.g. 9]. This is particular relevant to volcanic hazard assessments carried out at volcanoes near densely urbanized areas such as the Campi Flegrei caldera in southern Italy [16].

http://dx.doi.org/10.5772/51859

Several aligned edifices with the same eruption age may also be considered as a single volcanic event. Such vent alignments typically developed simultaneously as a result of magma supply from a single dike. For example the vent alignments in the Higashi-Izu monogenetic volcanic group [e.g. 35], could well be classified as a single volcanic event temporally but spatially are multiple. Where age data has been limited, some authors have implemented a condition whereby a cone or cones can only be defined as a volcanic event if they are associated with a single linear dike or a dike system with more complex geometry [e.g. 36].

Many of the advances made on modelling future spatial or spatio-temporal patterns of volcanism where carried out in monogenetic volcano fields due to the apparent relative ease of defining such volcanoes as point processes [e.g., 37, 38]. However as composite or established polygenetic volcanoes represent multiple eruptions from the same conduit occurring over several tens to hundreds of thousands of years, defining the volcanic event is not so easy if the focus is on single eruption episodes as the type of eruption can evolve significantly during the lifetime of the composite volcano. In fact the temporal definition of a monogenetic volcano appears to be not so straightforward either as this can range from several days to a few weeks or longer. For example the Ukinrek maar in Alaska formed in about eight days [39] and the 1913 eruption forming the Ambrym Volcano, Vanuatu in the south west pacific in just a few days [40]. Moreover, [41] argued that monogenetic volcanoes can be both spatially and temporarily more complex than a single eruptive event. In other words so called 'monogenetic' volcanoes can also be 'polygenetic' albeit smaller scaled than large volume complex strato or caldera volcanoes. Based on this there could be a case to look again at the volcanic event definition used in earlier probabilistic assessments carried out in monogenetic volcanic fields [e.g. 42, 43].

In Tohoku, new volcanoes forming at new locations typically evolve into large complex strato and/or caldera volcanoes containing multiple vents e.g. Akitakomagatake volcano [44]. Such large polygenetic volcanoes in Tohoku have been sub-grouped into unstable types where the eruptive centre has migrated more than 1.5 km within 10 ka and stable types were the vents are more concentrated around the geographic centre of the volcano [44].

The volcanic event definition requires information on both the temporal and spatial aspects; the temporal definition relates to the recurrence rate, λ_t(number of volcanic events per unit time), and spatial definition to the intensity or spatial recurrence rate $\lambda_{x,y}$ (number of volcanic events per unit area). $\lambda_t$and $\lambda_{x,y}$ can also be combined as a spatio-temporal recurrence rate $\lambda_{x,y,t}$ (number of volcanic events per unit area per unit time) [42].

The temporal definition of a volcanic event could range from a single eruption occurring in one day or less, to an eruption cycle in which active periods of eruptions occur between dormant periods. The time scale of an active period may vary from several years to thousands of years. In previous volcanic hazard analyses carried out on complex, large-volume strato and/or caldera volcanoes, volcanologists have typically defined volcanic events as single eruptions or several eruptions within some defined time period separated by periods in which there is no activity e.g. [4]. This is because the focus at such established volcanoes is not on the

probability of a new volcano forming in the vicinity of the existing volcano but rather on the probability of the next eruption or eruption phase.

3.1. Tohoku volcanic event definition

In the context of siting of a geological repository, the main concern is the formation of a new volcano in a region where volcanoes do not already exist. Thus the distinction between monogenetic (simple or complex) and polygenetic (complex strato and/or caldera) volcanism is not relevant for the definition of volcanic event here. Table 1 is a compilation of all Quaternary volcanoes in the Tohoku volcanic arc modified from the Catalog of Quaternary Volcanoes in Japan [1, 30]. Volcano complexes refer to magma systems that have evolved over the long-term (order of 0.1 Ma) which appear as regional scale clusters. In this chapter we use the same definition of volcanic event as [1] taking into account eruption volumes. This is depicted as a white triangle in Figure 3 and is the average geographic location of the vents (white dots). The eruption products released from the vents are represented by the dark grey regions in Figure 3. The lighter grey areas in Figure 3a are the eruption products of a separate volcanic event. Each volcanic event typically has a time gap of more than 10 ka, and/or is differentiated from other volcanic events according to geochemistry.

Volcano Complex	Volcanic event	Location		Age (Ma)			Dating Method	Eruptive volume
		Latitude	Longitude					(km³, DRE)
Mutsuhiuchi-dake	Older Mutsuhiuchi-dake	41.437	141.057		ca.0.73		K-Ar	5.9
Mutsuhiuchi-dake	Younger Mutsuhiuchi-dake	41.437	141.057	0.45		0.2	Strat.	3.6
Osorezan	Kamabuse-yama	41.277	141.123		ca.0.8		K-Ar	11.4
Hakkoda	Hakkoda P.F.1st.	40.667	140.897		0.65		K-Ar	17.8
Hakkoda	South-Hakkoda	40.600	140.850	0.65	—	0.4	K-Ar	52.4
Hakkoda	Hakkoda P.F.2nd.	40.667	140.897		0.4		K-Ar	17.3
Hakkoda	North-Hakkoda	40.650	140.883	0.16	—	0	K-Ar	30.4
Okiura	Aoni F. Aonigawa P.F.	40.573	140.763		ca.1.7		K-Ar	17.6
Okiura	Aoni F. Other P.F.	40.573	140.763	1.7	—	0.9	K-Ar	3.7
Okiura	Okogawasawa lava	40.579	140.759	0.9	-	0.65	Strat.	0.9
Okiura	Okiura dacite	40.557	140.755	0.9	-	0.7	K-Ar	2.1
Ikarigaseki	Nijikai Tuff	40.500	140.625		ca.2.0		K-Ar	20.2
Ikarigaseki	Ajarayama	40.490	140.600	1.91	—	1.89	K-Ar	2.1
Towada	Herai-dake	40.450	141.000					5.1
Towada	Ohanabe-yama	40.500	140.883	0.4	—	0.05	K-Ar	8.9
Towada	Hakka	40.417	140.867					1.4
Towada	Towada Okuse	40.468	140.888		0.055		14C	4.8
Towada	Towada Ofudo	40.468	140.888		0.025		14C	22.1

http://dx.doi.org/10.5772/51859

Volcano Complex	Volcanic event	Location		Age (Ma)			Dating Method	Eruptive volume
		Latitude	Longitude					(km³, DRE)
Towada	Towada Hachinohe	40.468	140.888		0.013		14C	26.9
Towada	Post-caldera cones	40.457	140.913	0.013	—	0	Strat.	14.4
Nanashigure	Nanashigure	40.068	141.112	1.06	—	0.72	K-Ar	55.5
Moriyoshi	Moriyoshi	39.973	140.547	1.07	—	0.78	K-Ar	18.1
Bunamori	Bunamori	39.967	140.717		1.2		K-Ar	0.1
Akita-Yakeyama	Akita-Yakeyama	39.963	140.763	0.5	—	0	K-Ar	9.9
Nishimori/Maemori	NIshimori/Maemori	39.973	140.962	0.5	—	0.3	K-Ar	2.6
Hachimantai/Chausu	Hachimantai	39.953	140.857	1	—	0.7	K-Ar	5.5
Hachimantai/Chausu	Chausu-dake	39.948	140.902	0.85	—	0.75	K-Ar	13.7
Hachimantai/Chausu	Fukenoyu	39.953	140.857		ca.0.7		Strat.	0.2
Hachimantai/Chausu	Gentamri	39.956	140.878					0.2
Yasemori/Magarisaki-yama	Magarisaki-yama	39.878	140.803	1.9	—	1.52	K-Ar	0.3
Yasemori/Magarisaki-yama	Yasemori	39.883	140.828		1.8		K-Ar	0.9
Kensomori/Morobidake	Kensomori	39.897	140.871		ca.0.8		Strat.	0.8
Kensomori/Morobidake	Morobi-dake	39.919	140.862	1	—	0.8	Strat.	2.5
Kensomori/Morobidake	1470m Mt. lava	39.909	140.872					0.1
Kensomori/Morobidake	Mokko-dake	39.953	140.857		ca.1.0		Strat.	0.5
Tamagawa Welded Tuff	Tamagawa Welded Tuffs R4	39.963	140.763		ca.2.0		K-Ar	83.2
Tamagawa Welded Tuff	Tamagawa Welded Tuffs D	39.963	140.763		ca.1.0		K-Ar	32.0
Nakakura/Shimokura	Obuka-dake	39.878	140.883	0.8	—	0.7	K-Ar	2.9
Nakakura/Shimokura	Shimokura-yama	39.889	140.933					0.4
Nakakura/Shimokura	Nakakura-yama	39.888	140.910					0.4
Matsukawa	Matsukawa andesite	39.850	140.900	2.6	—	1.29	K-Ar	11.6
Iwate/Amihari	Iwate	39.847	141.004	0.2	—	0	K-Ar	25.1
Iwate/Amihari	Amihari	39.842	140.958	0.3	—	0.1	K-Ar	10.6
Iwate/Amihari	Omatsukura-yama	39.841	140.919	0.7	—	0.6	K-Ar	3.3
Iwate/Amihari	Kurikigahara	39.849	140.882					0.2
Iwate/Amihari	Mitsuishi-yama	39.848	140.900		0.46		K-Ar	0.6
Shizukuishi/Takakura	Marumori	39.775	140.877	0.4	—	0.3	K-Ar	2.4
Shizukuishi/Takakura	Shizukuishi-Takakura-yama	39.783	140.893	0.5	—	0.4	Strat.	5.2
Shizukuishi/Takakura	Older Kotakakura-yama	39.800	140.900		1.4		K-Ar	2.7
Shizukuishi/Takakura	North Mikado-yama	39.800	140.875					0.3
Shizukuishi/Takakura	Kotakakura-yama	39.797	140.907	0.6	—	0.5	K-Ar	1.8
Shizukuishi/Takakura	Mikado-yama	39.788	140.870		ca.0.3			0.2

Volcano Complex	Volcanic event	Location		Age (Ma)			Dating Method	Eruptive volume
		Latitude	Longitude					(km³, DRE)
Shizukuishi/Takakura	Tairagakura-yama	39.808	140.878		ca.0.3			0.1
Nyuto/Zarumori	Tashirotai	39.812	140.827	0.3	—	0.2	K-Ar	0.6
Nyuto/Zarumori	Sasamori-yama	39.770	140.820	0.23	—	0.1	K-Ar	0.4
Nyuto/Zarumori	Yunomori-yama	39.772	140.827		ca.0.3			0.5
Nyuto/Zarumori	Zarumori-yama	39.788	140.850		0.56		K-Ar	0.9
Nyuto/Zarumori	Nyutozan	39.802	140.843	0.58	—	0.5	K-Ar	5.0
Nyuto/Zarumori	Nyuto-kita	39.817	140.855		ca.0.4		K-Ar	0.1
Akita-Komagatake	Akita-Komagatake	39.754	140.802	0.1	—	0	K-Ar	2.9
Kayo	Kayo	39.803	140.735	2.2	—	1.17	K-Ar	5.9
Kayo	KoJiromori	39.828	140.787		0.94		K-Ar	0.3
Kayo	Akita-Ojiromori	39.839	140.788	1.7	1.7	1.7	Strat.	0.3
Innai/Takahachi	Takahachi-yama	39.755	140.655	1.7	1.7	1.7	K-Ar	0.0
Innai/Takahachi	Innai	39.692	140.638	2	—	1.6	K-Ar	0.5
Kuzumaru	Aonokimori andesites	39.543	140.983		2.06		K-Ar	0.3
Yakeishi	Yakeishidake	39.161	140.832	0.7	—	0.6	K-Ar	9.5
Yakeishi	Komagatake	39.193	140.924		ca.1.0		K-Ar	7.6
Yakeishi	Kyozukayama	39.178	140.892	0.6	—	0.4	K-Ar	5.7
Yakeishi	Usagimoriyama	39.239	140.924	0.07	—	0.04	K-Ar	2.3
Kobinai	Kobinai	39.018	140.523	1	—	0.57	FT, K-Ar	2.3
Takamatsu/Kabutoyama	Kabutoyama Welded Tuff	39.025	140.618		1.16		TL	3.2
Takamatsu/Kabutoyama	Kiji-yama Welded Tuffs	39.025	140.618		0.30		K-Ar	5.1
Takamatsu	Takamatsu	38.965	140.610	0.3	—	0.27	K-Ar	3.8
Takamatsu	Futsutsuki-dake	38.961	140.661		ca.0.3			0.8
Kurikoma	Tsurugi-dake	38.963	140.792	0.1	—	0	K-Ar	0.2
Kurikoma	Magusa-dake	38.968	140.751	0.32	—	0.1	K-Ar	1.5
Kurikoma	Kurikoma	38.963	140.792	0.4	—	0.1	K-Ar	0.9
Kurikoma	South volcanoes	38.852	140.875		ca.0.5		K-Ar	0.3
Kurikoma	Older Higashi Kurikoma	38.934	140.779		ca.0.5		K-Ar	2.2
Kurikoma	Younger Higashi Kurikoma	38.934	140.779	0.4	—	0.1	K-Ar	0.7
Mukaimachi	Mukaimachi	38.770	140.520		ca.0.8		K-Ar	12.0
Onikobe	Shimoyamasato tuff	38.830	140.695	0.21	0.21	0.21	FT	1.0
Onikobe	Onikobe Centeral cones	38.805	140.727		ca.0.2		TL	1.1
Onikobe	Ikezuki tuff	38.830	140.695	0.3	—	0.2	FT	17.3
Naruko	Naruko Central cones	38.730	140.727		ca.0.045		14C	0.1
Naruko	Yanagizawa tuff	38.730	140.727		ca.0.045		FT	4.8

http://dx.doi.org/10.5772/51859

Volcano Complex	Volcanic event	Location		Age (Ma)		Dating Method	Eruptive volume
		Latitude	Longitude				(km³, DRE)
Naruko	Nizaka tuff	38.730	140.727	ca.0.073		FT	4.8
Funagata	Izumigatake	38.408	140.712	1.45	— 1.14	K-Ar	2.3
Funagata	Funagatayama	38.453	140.623	0.85	— 0.56	K-Ar	19.0
Yakuraisan	Yakuraisan	38.563	140.717	1.65	— 1.04	K-Ar	0.2
Nanatsumori	Nanatsumori lava	38.430	140.835	2.3	— 2	K-Ar	0.5
Nanatsumori	Miyatoko Tuffs	38.428	140.793	ca.2.5		Strat.	6.1
Nanatsumori	Akakuzure-yama lava	38.433	140.768	1.6	— 1.5	Strat.	1.5
Nanatsumori	Kamikadajin lava	38.447	140.772	1.6	— 1.5	K-Ar	0.8
Shirataka	Shirataka	38.220	140.177	1	— 0.8	K-Ar	3.8
Adachi	Adachi	38.218	140.662	ca.0.08		FT	0.9
Gantosan	Gantosan	38.195	140.480	0.4	— 0.3	K-Ar	4.6
Kamuro-dake	Kamuro-dake	38.253	140.488	ca.1.67		K-Ar	5.7
Daito-dake	Daito-dake	38.316	140.527				5.7
Ryuzan	Ryuzan	38.181	140.397	1.1	— 0.9	K-Ar	4.6
Zao	Central Zao 1st.	38.133	140.453	1.46	— 0.79	K-Ar	0.8
Zao	Central Zao 2nd.	38.133	140.453	0.32	— 0.12	K-Ar	15.2
Zao	Central Zao 3rd.	38.133	140.453	0.03	— 0	K-Ar	0.0
Zao	Sugigamine	38.103	140.462	1		K-Ar	9.9
Zao	Fubosan/byobudake	38.093	140.478	0.31	— 0.17	K-Ar	15.2
Aoso-yama	Gairinzan	38.082	140.610	0.7	— 0.4	K-Ar	6.1
Aoso-yama	Central Cone	38.082	140.610	0.4	— 0.38	K-Ar	3.0
Azuma	Azuma Kitei lava	37.733	140.247	1.3	— 1	K-Ar	24.7
Azuma	Higashi Azumasan	37.710	140.233	0.7	— 0	K-Ar	22.8
Azuma	Nishi Azumasan	37.730	140.150	0.6	— 0.4	K-Ar	7.2
Azuma	Naka Azumasan	37.713	140.188	0.4	— 0.3	K-Ar	4.6
Nishikarasugawa andesite	Nishikarasugawa andesite	37.650	140.283	ca.1.5		K-Ar	1.9
Adatara	Adatara Stage 1	37.625	140.280	0.55	— 0.44	K-Ar	0.3
Adatara	Adatara Stage 2	37.625	140.280	ca.0.35		K-Ar	0.4
Adatara	Adatara Stage 3a	37.625	140.280	ca.0.20		K-Ar	2.0
Adatara	Adatara Stage 3b	37.625	140.280	0.12	— 0.0024	K-Ar	0.3
Sasamori-yama	Sasamari-yama andesite	37.655	140.391	2.5	— 2	K-Ar	0.4
Bandai	Pre-Bandai	37.598	140.075	ca.0.7		K-Ar	0.1
Bandai	Bandai	37.598	140.075	0.3	— 0	Strat.	14.0
Nekoma	Old Nekoma	37.608	140.030	1	— 0.7	K-Ar	11.4
Nekoma	New Nekoma	37.608	140.030	0.5	— 0.4	K-Ar	0.9

Volcano Complex	Volcanic event	Location		Age (Ma)			Dating Method	Eruptive volume
		Latitude	Longitude					(km³, DRE)
Kasshi/Oshiromori	Kasshi	37.184	139.973					0.1
Kasshi/Oshiromori	Oshiromori	37.199	139.970					0.7
Kasshi/Oshiromori	Matami-yama	37.292	139.886					0.3
Kasshi/Oshiromori	Naka-yama	37.282	139.899					0.0
Shirakawa	Kumado P.F.	37.242	140.032		1.31		K-Ar	19.2
Shirakawa	Tokaichi A.F. tuffs	37.242	140.032	1.31	—	1.24	Strat.	12.0
Shirakawa	Ashino P.F.	37.242	140.032		1.2		FT	19.2
Shirakawa	Nn3 P.F.	37.242	140.032	1.2	—	1.17	Strat.	0.0
Shirakawa	Kinshoji A.F. tuffs	37.242	140.032	1.2	—	1.18	Strat.	9.0
Shirakawa	Nishigo P.F.	37.252	139.869		1.11		FT	28.8
Shirakawa	Tenei P.F.	37.242	140.032		1.06		Strat.	7.7
Nasu	Futamata-yama	37.244	139.971		0.14		K-Ar	3.2
Nasu	Kasshiasahi-dake	37.177	139.963	0.6	—	0.4	K-Ar	12.3
Nasu	Sanbonyari-dake	37.147	139.965	0.4	—	0.25	K-Ar	5.5
Nasu	Minamigassan	37.123	139.967	0.2	—	0.05	K-Ar	8.7
Nasu	Asahi-dake	37.134	139.971	0.2	—	0.05	K-Ar	4.6
Nasu	Chausu-dake	37.122	139.966	0.04	—	0	K-Ar	0.3
Chokai	Shinsan Lava flow	39.097	140.053	0.02	—	0	Strat.	
Chokai	Higashi Chokai	39.097	140.053	0.02	—	0.02	K-Ar	4.3
Chokai	Nishi Chokai	39.097	140.020	0.09	—	0.02	Stra.	0.8
Chokai	Nishi ChokaiII	39.097	140.020	0.13	—	0.01	K-Ar	21.0
Chokai	Old Chokai	39.103	140.030	0.16	—	0.55	K-Ar	67.0
Chokai	Uguisugawa Basalt	39.103	140.030	0.55	—	0.6	K-Ar	1.0
Chokai	Tengumari volcanics	39.103	140.031	0.55	—	0.6	K-Ar	11.0
Gassan	Ubagatake	38.533	140.005	0.400	—	0.300	K-Ar	3.5
Gassan	Yudonosan lavas/ pyroclastics	38.534	139.988	0.800	—	0.700	K-Ar	7.5
Gassan	Gassan	38.550	140.020	0.500	—	0.400	K-Ar	18.0
Numazawa	Sozan lava domes	37.452	139.577					
Numazawa	Mizunuma pyroclastic dep.	37.452	139.577		ca.0.05		FT	2.0
Numazawa	Numazawa pyroclastics	37.452	139.577	0.005	—	0.005	14C	2.5
Numazawa	Mukuresawa lava	37.452	139.577		—			
Ryuzan	Ryuzan	38.181	140.397	1.130	—	0.940	K-Ar	6.0
Sankichi-Hayama	Sankichi-Hayama	38.137	140.315	2.400	—	2.300	K-Ar	2.9
Daitodake	Daitodake	38.316	140.527		ca.1		Strat.	7.5

http://dx.doi.org/10.5772/51859

Volcano Complex	Volcanic event	Location		Age (Ma)			Dating Method	Eruptive volume
		Latitude	Longitude					(km^3, DRE)
Hijiori	Hijiori Pyroclastic flow	38.610	140.159		ca.0.01		Strat.	1.0
Hijiori	Komatsubuchi lava dome	38.613	140.171		ca.0.01		Strat.	0.0
Tazawa	Tazawa (lake)	39.723	140.667					
Daibutsu	Daibutsu	39.817	140.517	2.340	—	2.160	K-Ar	3.2
Kampu	Kampu	39.928	139.877	0.030	—	0.000	Strat.	0.6
Toga	Toga	39.950	139.718		ca.0.42		FT/K-Ar	2.0
Megata	Megata	39.952	139.742	0.030	—	0.020	Strat.	0.1
Inaniwa	Inaniwa	40.195	141.050	7.000	—	2.700	K-Ar	14.0
Taira-Komagatake	Taira-Komagatake	40.410	140.254	0.200	—	0.170	Strat.	3.0
Tashiro	Tashiro	40.425	140.413	0.600	—	0.470	K-Ar	9.0
Tashiro	Hirataki nueeardente deps.	40.420	140.413	0.020	—	0.020	Strat.	0.7
Iwaki	Iwaki	40.653	140.307	0.330	—	0.000	K-Ar	49.0

Table 1. Tohoku volcanic arc [30, 28]. Dense-rock equivalent (DRE) of eruptive volumes is the product of volume and density of the respective volcanic deposits.

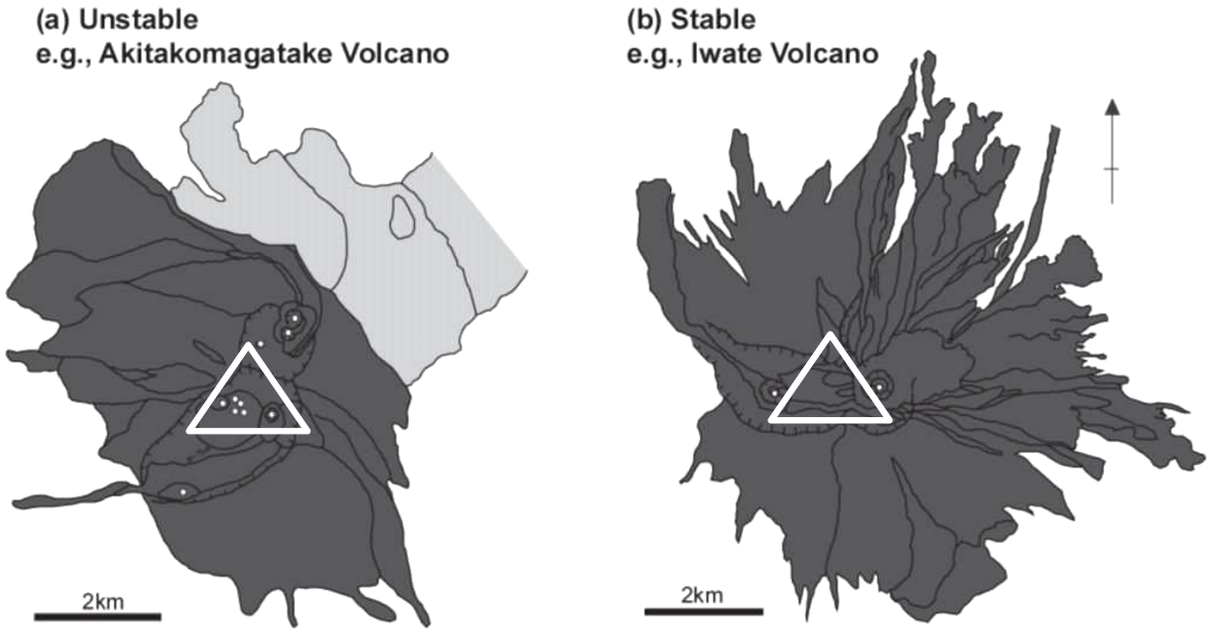

Figure 3. Two volcano types in Tohoku classified according to migration distance from eruption centre [44]: (a) an unstable type with vent (white dots) migration exceeding 1.5 km in 10 ka resulting in a summit with multiple peaks; and (b) a stable type commonly with a narrow saw-tooth or pointed appearance. For consistency in volcanic event definition over the Tohoku region, both types are treated as a single volcanic event (white triangle) in the probability analysis. However they are also optionally weighted with the corresponding eruption products (dark grey regions). (Figure modified from [1]).

4. Bayesian model

The following is a slightly shorter description of the Bayesian methodology published in [1]. A two-dimensional surface distribution is set-up showing the continuous probability of one or more volcanic event(s) forming within a region of interest, in an arbitrarily time frame of the order of 0.1 – 1 Ma. The volcanic event definition defined above means that we are estimating with known uncertainty, the probability of a new volcano forming at a given location (x, y). [1] noted that a challenge with estimating the long-term future spatial distribution of volcanism is the fact that we are trying to model something that we cannot sample directly; namely the locations of future volcanoes. In this chapter we incorporate $^{3}He/^{4}He$ ratios, as these may be indicative of conduits in the earth's crust through which magma may rise through resulting in future volcano formation [19, 20].

Information, no matter how obtained, can be described by a probability density function (PDF) [e.g. 45, 46]. Once the dataset is expressed as a PDF, it is possible to combine with our initial PDF created based on *a priori* assumptions on volcanism. Bayesian inference is a powerful tool that allows us to construct an a *posteriori* PDF given *a priori* assumptions and the PDF generated by our new dataset.

Essentially, two stages are performed yielding the *a posteriori* PDF. The first is to make a long-term future prediction based solely on the distribution and ages of past volcanic events, creating an *a priori* PDF. The *a priori* assumption is that the past and the present provide information about the future; in other words the locations of past and present volcanism are used as an initial guide to estimating future long-term spatial patterns of volcanism. The basic logic behind the *a priori* assumption is that a new volcano doesn't form far from existing volcanoes. The *a priori* assumption can be quite vague in the first step as it is simply the starting point. The next stage is to update or modify the *a priori* assumptions by incorporating information that is likely to be indicative of the locations of future volcanism and/or we have increased our understanding of the process that controls the location of volcanism. This new information and/or knowledge, obtained from chemical and/or geophysical data, is used to modify the *a priori* PDF to form an *a posteriori* PDF that is expected to better reflect the location of future volcanism. The cycle can be repeated any number of times for other datasets by treating the *a posteriori* PDF as the new *a priori* PDF in the first step above.

4.1. Bayesian inference and Bayes' theorem

Bayes' theorem [e.g. 47] is used to setup a model providing a joint probability distribution for the location known volcanic events (*a priori* PDF) and current R/R_A contoured datasets recast as a PDF (likelihood function). The joint probability density function or *a posteriori* PDF can be written as the product of two PDFs; the *a priori* PDF and the sampling or likelihood PDF

$$\mathbf{P}(x,y \mid \theta) = \frac{\mathbf{P}(x,y)\mathbf{L}(\theta \mid x,y)}{\int_A \mathbf{P}(x,y)\mathbf{L}(\theta \mid x,y)dA} \tag{1}$$

http://dx.doi.org/10.5772/51859

where x and y represent grid point locations within the volcanic field A, $\theta$is additional dataset, $\boldsymbol{P}(x, y)$is the *a priori* PDF, $\boldsymbol{L}$ $(\theta \mid x, y)$the likelihood function generated by conditioning additional data on the locations of volcanic events, and $\boldsymbol{P}(x, y \mid \theta)$ the resulting *a posteriori* PDF [1]. The *a posteriori* PDF is normalized to unity by integrating over the entire Tohoku volcanic field; hence total cumulative probability will not change but the shape of the 2-D surface distribution will be modified according to the likelihood function.

4.2. A priori PDF

We assume that past and present volcanic events can be used to estimate future locations of volcanoes over the long-term, as well as constraining upper bound recurrence rates in the volcanic field. The spatial distribution of volcanoes in volcanic arcs like Tohoku are random [48] hence by treating volcanism in Tohoku volcanic arc as a low frequency, random event, it is assumed that the underlying process could be approximated to a Poisson process [1]. Moreover, by treating the location of volcanic events as random points within some set, the spatial distribution of volcanism can be modeled as a spatial point process [1] where a spatial point process is a stochastic model that can be described as the process controlling the spatial locations of the events$\boldsymbol{s}_1,\ldots,\boldsymbol{s}_1$ in some arbitrary set $\boldsymbol{S}$ [49]. In applying point process models to volcanism, [42] eloquently defined$\boldsymbol{s}_1,\ldots,\boldsymbol{s}_n$ as volcanic events and $\boldsymbol{S}$ as the volcanic field.

The Poisson process is 'homogeneous' if the spatial distribution of point events are completely random [49]. However, as with many volcanic fields, spatial patterns of volcanism in the Tohoku volcanic arc are clustered [34, 50], hence the distribution of volcanoes are not completely random and therefore non-homogeneous (also referred to as in-homogenous). Applying the Clark-Evans nearest-neighbour test [51], [1] showed that the distribution of the volcanic events defined above is clustered with greater than 95% confidence. A non-homogeneous Poisson process is the simplest alternative for modeling such clustered events. Moreover, point process models based on non-homogeneous Poisson processes have been extensively used in modeling the spatial and spatio-temporal characteristics of several volcano fields (e.g. the Springerville volcanic fields in Arizona [38] and the Higashi-Izu monogenetic volcano group, Shizuoka Prefecture, Japan [43]. In these models the local spatial density of volcanic events $\lambda_{x,y}$ is calculated using a kernel function [37, 52]. The kernel function itself is a density function used to obtain the intensity of volcanic events at a sampling pointx_p, y_p, calculated as a function of the distance to nearby volcanoes and a smoothing constant h (Figure 4).

As noted by [42] the choice of kernel function with appropriate values of h has some consequence for the parameter estimation because it controls how $\lambda_{x,y}$ varies with distance from existing volcanoes. The Gaussian kernel has been used a lot in probabilistic assessments carried out in monogenetic volcanic fields, [e.g. 15, 43] since it was assumed that the next volcano to form would not be far from an existing volcanoes. In order to include extreme volcanic events further afield however, [1] modelled spatial patterns using the Cauchy kernel which has thicker tails than the Gaussian kernel. [1] also showed that the spatial distribution of volcanic events in the Tohoku volcanic arc fit a Cauchy distribution whereas monogenetic fields such as the Higashi-Izu Monogenetic Volcano Group [43] tend to be Gaussian. We

therefore also use a two-dimensional Cauchy kernel here to calculate the spatial recurrence rate $\lambda_{x,y}$ at grid point x_p, $y_p$where:

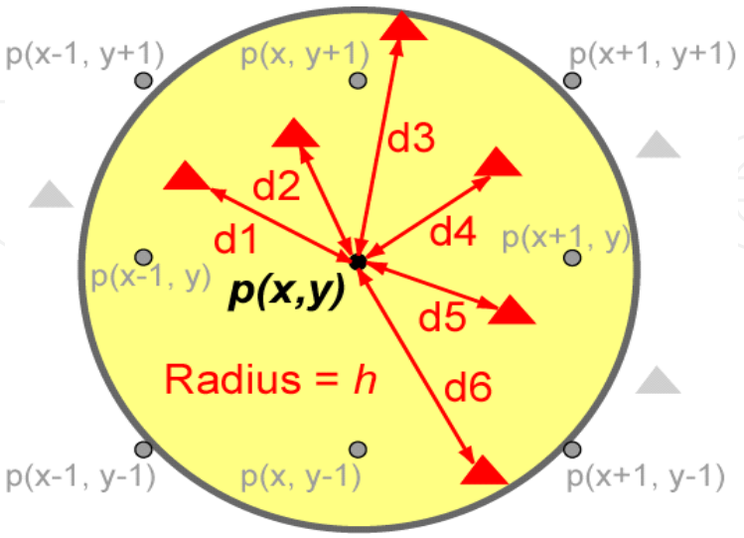

Figure 4. Local volcano intensity $\lambda_{x,y}$ at each grid point (x, y) is computed using a Cauchy kernel function. $\lambda_{x,y}$is a function of volcano distance from grid point (x, y) for $N = 6$ volcanoes (modified from [1]).

$$\lambda_{x,y} = \frac{1}{\pi h^2 N} \sum_{i=1}^{N} \left\{ \frac{l_{vi}}{1 + \left[\left(\frac{x_p - x_{vi}}{h} \right)^2 + \left(\frac{y_p - y_{vi}}{h} \right)^2 \right]} \right\} \tag{2}$$

x_{vi}, $y_{vi}$are Cartesian coordinates of the ith volcanic event, N the number of volcanic events used in the calculation and l_{vi} is a factor for weighting eruption volume of the corresponding ith volcanic event. $l_{vi}$is set to unity when eruption volume is excluded. The calculation is repeated on a 10 km mesh in the study area 139 to 143 longitude and 37 to 41.6 latitude and the resulting PDF is normalized to unity. The 10 km grid spacing was selected taking into account the resolution of available geophysical or geochemical datasets across the entire Tohoku volcanic arc.

4.3. Estimating an optimum smoothing coefficient h for the volcanoes in Tohoku

The choice of the smoothing coefficient depends on a combination of the size of the volcanic field, size and degree of clustering and the amount of robustness and conservatism required at specific points within or nearby the volcanic fields in question. In order to estimate the most likely optimum value of smoothing coefficient, [1] plotted cumulative probability density

http://dx.doi.org/10.5772/51859

functions with varying values of smoothing are compared with the fraction of volcanic vents and nearest-neighbour volcanic event distances in Tohoku (Figure 5).

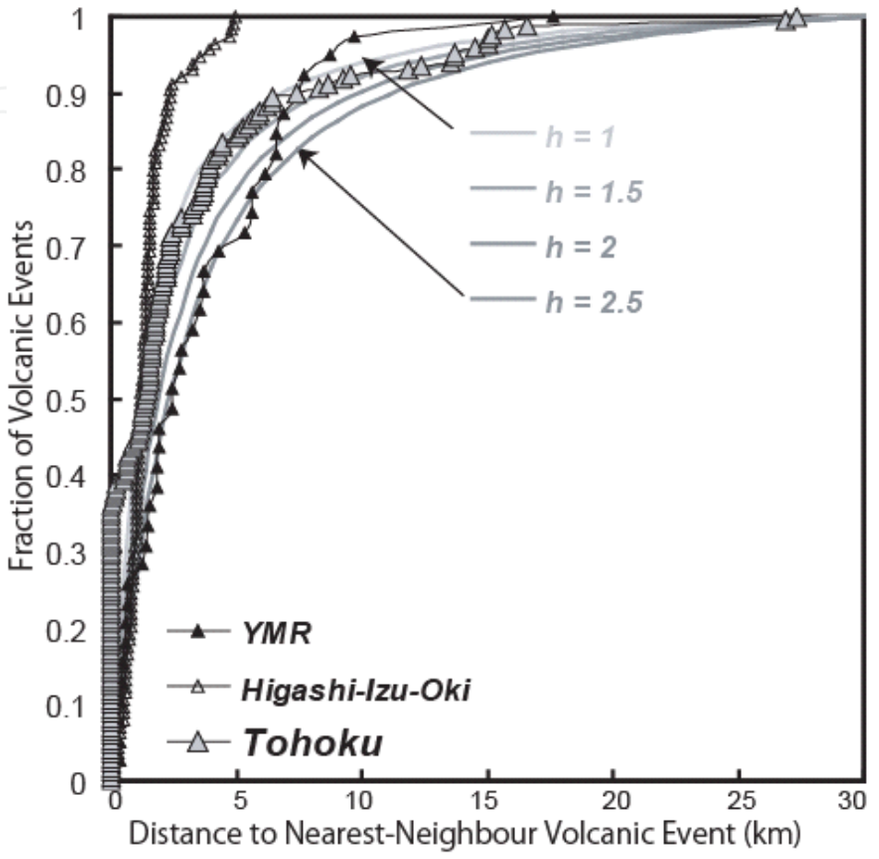

Figure 5. Suitable values of smoothing coefficient *h* are estimated by plotting cumulative distances to nearest neighbour volcanic events and cumulative probability distribution with differing values of smoothing coefficient. From this plot, suitable values of smoothing coefficient for known volcanic events in Tohoku volcanic are estimated to be 1-1.5 km for the Cauchy kernel. (Figure modified from [1]). As a comparison, the monogenetic volcanoes in the Yucca Mountain Region (YMR) and the Higashi-Izu-Oki monogenetic volcano group are also plotted.

The cumulative plots in Figure 5 suggest that the spatial distribution of volcanic events in the Tohoku volcanic arc fit a Cauchy distribution with smoothing coefficients of $h = 1$–1.5 km.

4.4. A priori probabilities

Probability estimates for each grid point x_p, y_p are computed by using a Poisson distribution where $\lambda_{x,y}$ represents the intensity parameter computed using equation (2) :

$$P_{x,y}\{N(t) \geq 1\} = 1 - \exp\left(-t\lambda_t \lambda_{x,y} \Delta x \Delta y\right) \tag{3}$$

where, $N(t)$ represents the number of future volcanic vents that occur within time t and area $\Delta x \Delta y$ (10 km x 10 km). The parameter $\lambda_{x,y}$ is normalized to unity across the Tohoku, so, equation (3) represents the probability of one or more volcanic event(s) forming in an area $\Delta x \Delta y$ centred on point x_p, y_p given the formation of a new volcanic event in Tohoku. This calculation is repeated on a grid throughout Tohoku. The resolution is such that the spatial recurrence rate $\lambda_{x,y}$ does not vary within each cell. For the regional recurrence rate λ_t an average of 120 volcanic events per million years is used, effectively taking average Quaternary activity [1].

Using smoothing coefficients of 1 - 1.5 km for the Cauchy kernel, as well as weighting eruption volumes, probability plots were constructed using equation (3). A probability contour plot for one case is shown in Figure 6.

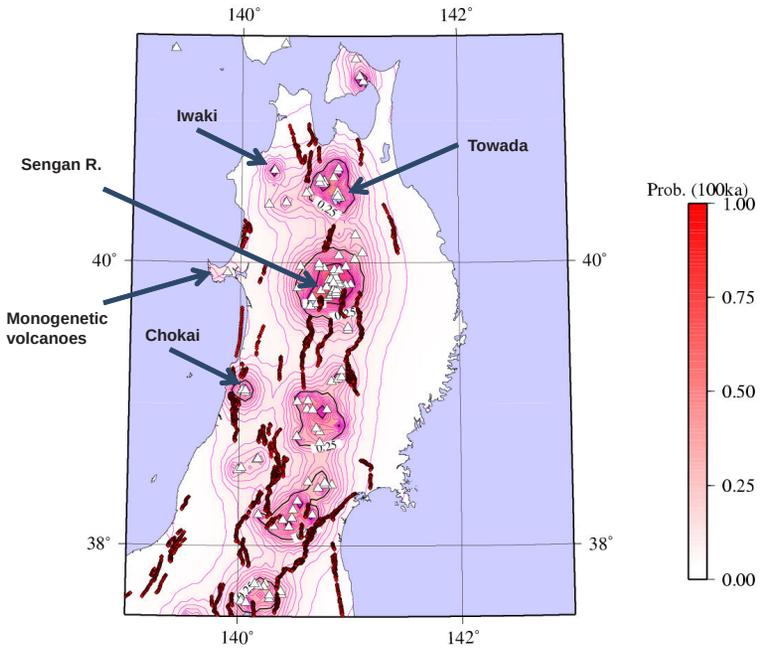

Figure 6. Probabilities of one or more volcanic events occurring in the next 100 ka based on *a priori* PDF (Cauchy (h = 1.5 km). White triangles denote the volcanic events used in the calculation and black lines are active faults [35]

The highest probabilities are located in the Sengan region (10^{-6} - 10^{-5} / a) which has the highest density of volcanic events in the Tohoku volcanic arc. By testing the two volcanic event sub-definitions (weighted with and without eruption volume), [1] found that the probabilities in the vicinity of monogenetic volcanoes on the back-arc region were higher when volcanic events were not weighted with eruption volumes (1 - 4 x 10^{-7}/a, weighted; 1 - 4 x 10^{-6}/a, unweighted), whereas the probabilities around established centers such as Iwaki, Towada, Sengan and Chokai were reduced slightly. This is expected as volcanoes with large eruption volumes are the sites of highest magma production. However if the focus of the assessment is on new volcano event formation, irrelevant of whether the new volcano evolves into are large complex stratovolcano and/or caldera or not, then selecting the volcanic event definition that is not weighted with eruption volume would seem more appropriate.

http://dx.doi.org/10.5772/51859

4.5. The likelihood function

Here the *a priori* PDF is conditioned $^3He/^4He$ ratios. This is done by normalizing additional data into a likelihood function according to how such information is judged by the expert and/or indicated by experimental result to relate to the distribution of volcanism [1]. Helium isotopes have been shown to provide evidence for the presence of mantle derived materials in the crust, and hence potential volcanism based on distinct $^3He/^4He$ ratios (Figure 7) [17, 18]. [1] looked at seismic tomographs and geothermal gradients. This is because *P* velocity perturbations ($\Delta V / V$) in particular at 40 km depth [29] is a good estimate of the minimum depth of partial melting in the mantle for most of the volcanoes in Tohoku. Geothermal gradients on the other hand were used by [1] as an additional aid to *P* velocity perturbations since it is not possible to differentiate heat from *P* wave velocity alone.

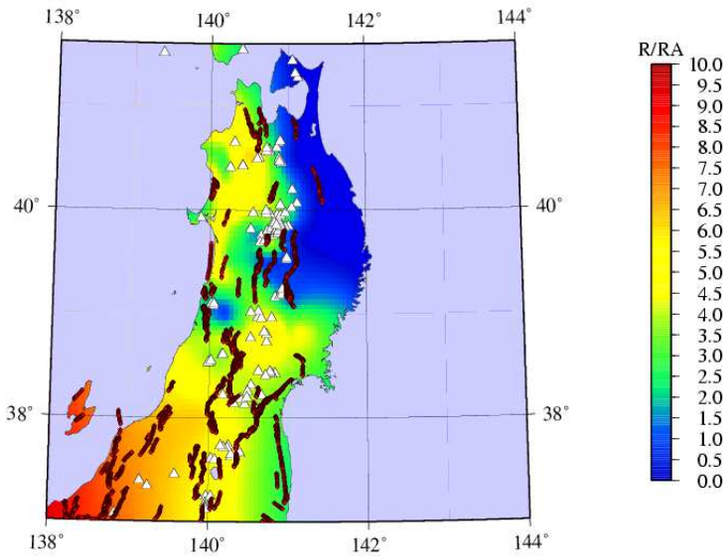

Figure 7. Distribution of R/R_A data (Ra denotes the atmospheric $^3He/^4He$ ratio of 1.4×10^{-6}) taken from boreholes and hot springs [20, 54, 55]

In order to compare the R/R_A ratios, cumulative plots of values around all volcanic events and values of 10 km^2 bins over all of Tohoku are plotted. Figure 8 shows R/R_A ratios below all volcanic events (8a) and volcanic events less than 100 ka (8b). In both cases approximately 90% of all volcanic events are distributed in regions with R/R_A ratios greater than 3. In other words 90% volcanoes are located in regions where $^3He/^4He$ is elevated.

The R/R_A ratios are interpolated to represent a continuous, differentiable surface and then the spatial data are mapped into a likelihood function based on the percentage of recent volcanic events that lie within the binned R/R_A ratios in Figure 8. For low P velocity perturbation, [1] assumed an inverse linear relationship; based on the interpretation that low *P* velocity perturbation corresponds to partial melting (and hence increased probability of volcanism). In this case, 10% of volcanoes less than 100 ka located in regions where $\Delta V / V$ ranged from -6% to -5% etc. For geothermal gradients [1] used a linear relationship for recasting the data values as a PDF.

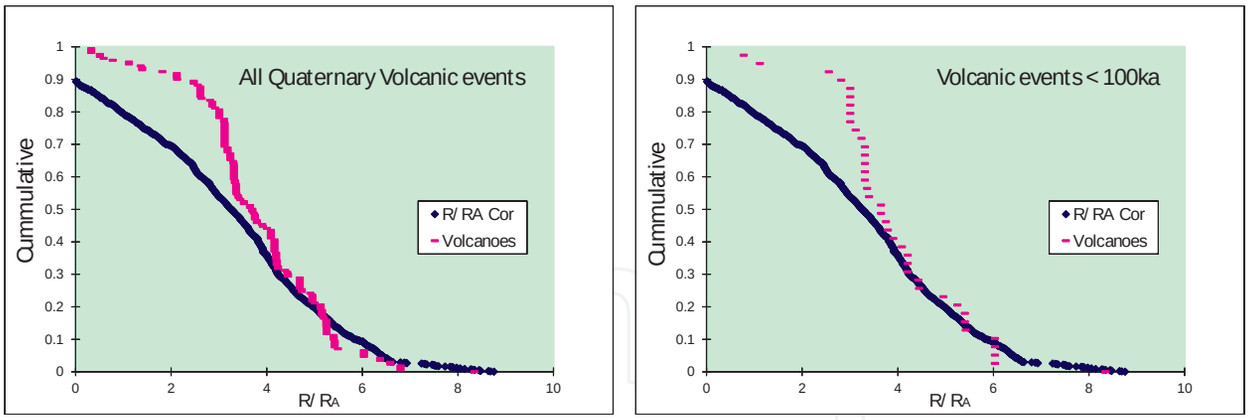

Figure 8. umulative plots of R/R_A values below volcanic events and the whole of Tohoku (10km^2 grid spacing).

4.6. A posteriori probabilities

Finally the *a posteriori* PDF is calculated from the likelihood function and the *a priori* PDF using equation (1). The integral across the entire field of both the *a priori* and the *a posteriori* PDFs is set to unity; however the shape of the distribution is modified by the likelihood function. The probability of a new volcanic event is calculated for each grid point using equation (3).

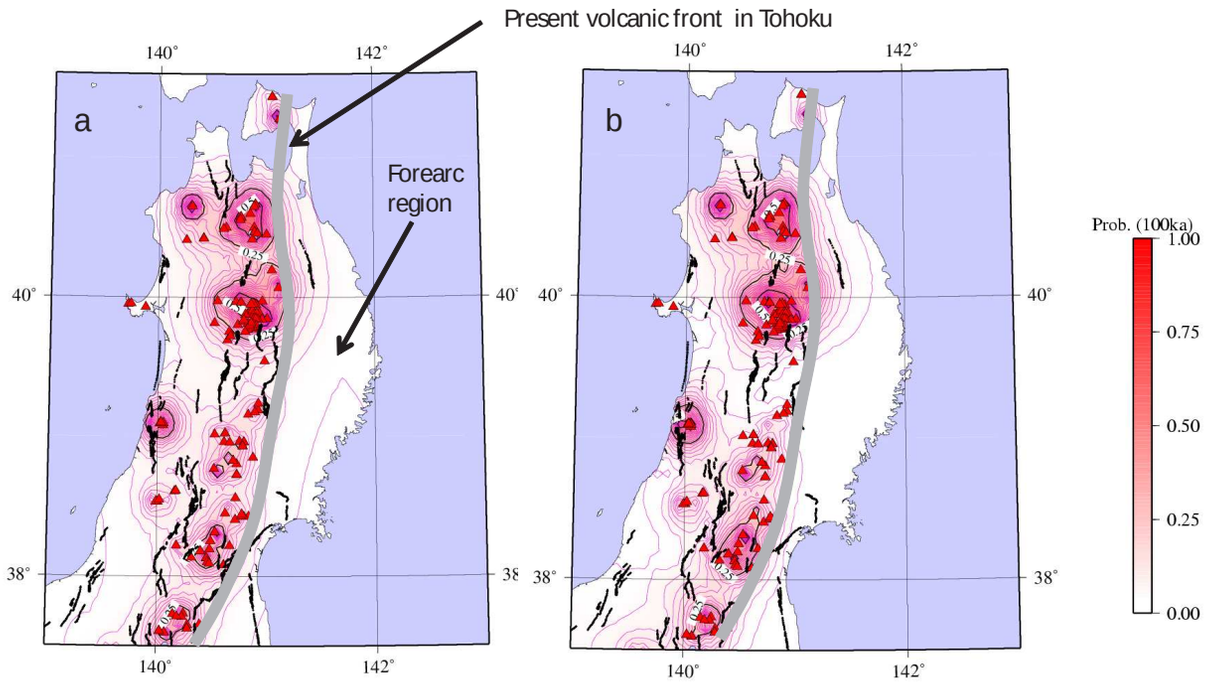

Figure 9. Comparison of *a priori* (a) and *a posteriori* probability plots (b) calculated with a Cauchy kernel (h = 1.5 km) conditioned on R/R_A ratios. Both PDFs a weighted by eruption volume. Black lines are active faults [53].

Using equations (1) to (3) above, two dimensional probability plots are subsequently constructed showing the probability of one or more future volcanic event(s) forming during the

http://dx.doi.org/10.5772/51859

long-term, given that a volcanic event will occur in the Tohoku volcanic arc during 100 ka. Figure 9 shows a comparison of the *a priori* probability (9a) and a posteriori probability (9b) conditioned on R/R_A ratios of one or more volcanic events forming in 100 ka.

The probability of new volcanic event formation in the forearc region to the east of the volcanic front is reduced slightly in the *a posterior* probability calculation. This is more evident when we repeat the calculation for new volcanic events forming in the next 1Ma (Figure 10).

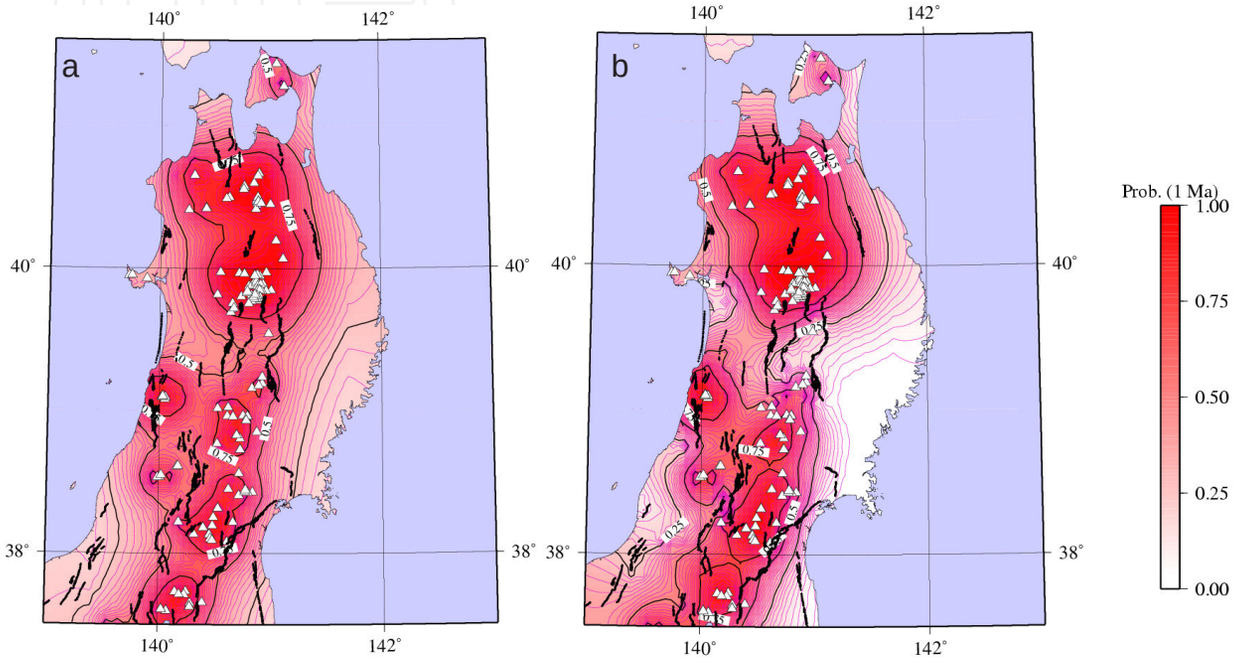

Figure 10. Probability of the formation of a new volcanic event over the next 1Ma; *a priori* (a) and *a posteriori* (b) probability plots calculated with a Cauchy kernel (h = 1.5 km) conditioned on R/R_A ratios.

The R/R_A analyses are compared with the probability calculations conditioned on *P* velocity perturbations (10 or 40 km) (Figure 11) and geothermal gradients (Figure 12) [1]. The *a posteriori* probability below Iwaki volcanic event is particularly low when conditioned on 40 km depth P velocity perturbation datasets but that there was no significant change beneath Chokai, another andesitic volcano on the back-arc side of Tohoku. With the *a posteriori* calculation conditioned on the R/R_A analyses, no decrease is seen in the probabilities below Iwaki volcano when compared to *a priori* plots. Similar results can be seen when probabilities are conditioned on 10km depth P velocity perturbations (Figure 11a) or geothermal gradients (Figure 12) [1].

[1] found that *a posteriori* probabilities are not reduced when compared to *a priori* probabilities in the northern regions when conditioning on shallower (10 km) *P* velocity perturbations or on geothermal gradients. This seems reasonable as seismic velocity structure [57] and the depth of Curie isotherms [58] in this part of Tohoku reveal high-temperature-like geophysical anomalies at depths of up to 10 km below Iwaki volcano which may be indicative of the shallower depths (ca. 10km) of magma chambers.

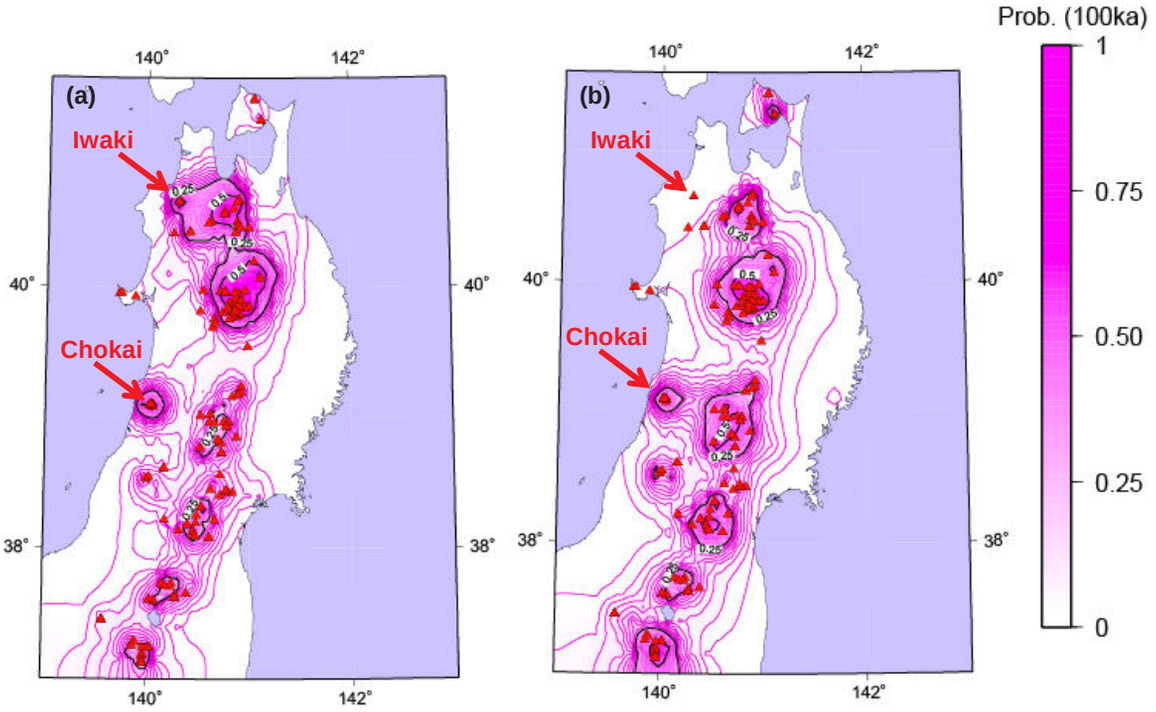

Figure 11. *A posteriori* probability plots calculated with: (a) Cauchy kernel (h = 1.5 km) conditioned on $\Delta V / V$ at 10 km depth; (b) Cauchy kernel (h = 1.5 km) conditioned on $\Delta V / V$ at 40 km depth (modified from [1]).

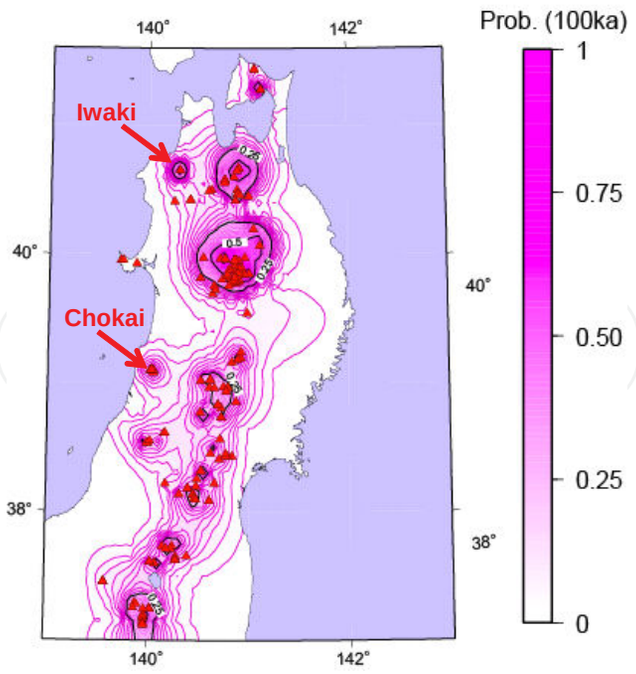

Figure 12. *A posteriori* probability plots calculated with Cauchy kernel (h = 1.5 km) conditioned on geothermal gradients (modified from [1])

http://dx.doi.org/10.5772/51859

5. Discussion

The main advantage of probabilistic based models over deterministic models is that the probability of new volcano event formation is never zero. [1] showed that Bayesian inference is well-suited for formally combining observations relevant to the imaging of the magma source region (e.g. seismic tomography) with quantitative methods for estimation of volcano intensity. Moreover, the strength of Bayesian inference is that probabilistic assessments can be improved with increased understanding of the physical processes governing magmatism and/or data that may be indicative of future volcanism such as the helium isotope ratios presented here. Nevertheless it is worth examining the logic behind what we perceive to be 'data' and what we mean by *a priori* information and knowledge.

5.1. Which datasets are a priori information?

[1] used the volcano geographical datasets themselves as a starting point in their analysis. The same approach was applied in this chapter. In the first step a Cauchy kernel was used to calculate$\lambda_{x,y}$. This means that the probability new volcanic event formation decreases with increasing distance from existing volcanic events. In the case of selecting a location for a geological repository, there may be a need to have a conservative estimate and accept that extreme events may occur. In this case, selection of the Cauchy as the *a priori* PDF would be most appropriate due to the thickness of the tails. This is especially the case if we have to make probability calculations for periods for 1Ma where the tectonic setting can change, and we may have a shift in the location of the volcanic front. The probabilities in distal regions would only be reduced in the *a posterior* probability calculation if newly obtained evidence in such regions shows that volcano formation is zero or close to zero. Since R/R_A ratios vary due to the heterogeneous release of mantle helium and elevated ratios and are likely to indicate the presence of partial melting [e.g. 20] datasets may give some indication on the future location of volcanism even in non-volcanic regions. Seismic tomography on the other hand offers a direct view of the mantle that can be interpreted in terms of degree of partial melting [e.g. 58, 59].

It could be equally argued, however that the logic of [1] should be reversed in that the models based on seismic tomography or elevated helium isotope ratios are in fact *a priori* information or knowledge, and the location of volcanic events the 'data'. The philosophy here is that we assume new volcanic events will form in regions where partial melting is likely to be occurring now and that the distribution of known volcanic events are the datasets updating our model and/or knowledge. However, this may be true for the very recent volcanism up to about 1,000 years say, but how relevant are volcanic events that formed over 100,000 years ago or more to the present day geophysical snap-shot of the Earth's crust or upper mantle? This question is difficult to answer as there is very little information on the temporal behaviour of partial melting in the mantle. This is also evident when we try to evaluate our forecasts below. A problem here is that we are always trying to predict the formation of future volcanic events which may or may not be related to historic volcanic events. Our closest 'data' to such future events are thus present day geophysical snap shots of the current conditions in the crust or

upper mantle and/or newly formed or forming volcanic events. This has been the motivation for [1] to use such geophysical data or models as the basis of the likelihood function.

On the other hand there are also practical aspects to be considered particularly when starting a hazard analysis in a region where there have not been many studies. In such a case, the only data available to begin with might be just the geographical location of volcanoes. Information from more complicated and expensive surface based investigations might not come until later.

5.2. Model evaluation

Since it is not possible to infer directly the location of future volcanic events that will form in the next 0.1 to 1 Ma from now, models can instead by evaluated by calculating the probability of the new volcanic events that formed after some time in the past, using all volcanic events that formed before that time [1, 38]. Since we calculate the probability of future volcanism in the next 100 ka in most of the analyses described here, 100 ka is selected as the timeframe in the verification calculations. In Tohoku, as there are a large number of dated volcanic events it is possible to verify the Bayesian models developed to a certain extent by using all volcanic events that formed before 100 ka to predict the location of volcanic events that formed between 100 ka and the present day. Since the 'new' volcanic events are still in the past, it is possible to compare probability plots with the locations of volcanic events we are attempting to forecast. Figure 13 shows probability plots for the Cauchy PDF (h=1.5 km) and the *a posterior* probability conditioned on R/R_A ratios. All volcanic events that formed before 100 ka (white triangles) during the Quaternary were used to make a forecast for the period from 100 ka ago to the present day. All subsequent volcanic events that formed during the forecast period are shown in red. Probability calculations are then compared with the locations of volcanoes that formed during the forecast period.

In both cases, all subsequent volcanoes formed in regions where the probability was at least 10%. Approximately 50% of newly formed volcanic events formed in regions where the probability was at least 25%. There was approximately 10% increase in probabilities in the locations were volcanoes formed in the *a posteriori* probability calculations.

Probability calculations above were made using single inferences on one set of data. However, Bayes' theorem allows beliefs to be updated as additional information becomes available. [1] attempted this by combining geothermal and seismic tomography datasets (Figure 14).

By conditioning on *P* velocity perturbations at 40 km depth, the model assigned a low probability for the Iwaki volcano which formed in region where probability was calculated to be low ($< 10^{-9}$/a). This could be improved upon by including both P velocity perturbations at 10 km depth and geothermal gradients [1].

5.3. Varying the temporal recurrence rate

The temporal recurrence rates in Tohoku have been steady state from 0.5 Ma to present [28]. This implies that recurrence rates are likely to remain steady state for at least the next 0.1 Ma. However if we need to assess volcanism over a much longer time frame such as 1.0 Ma more

http://dx.doi.org/10.5772/51859

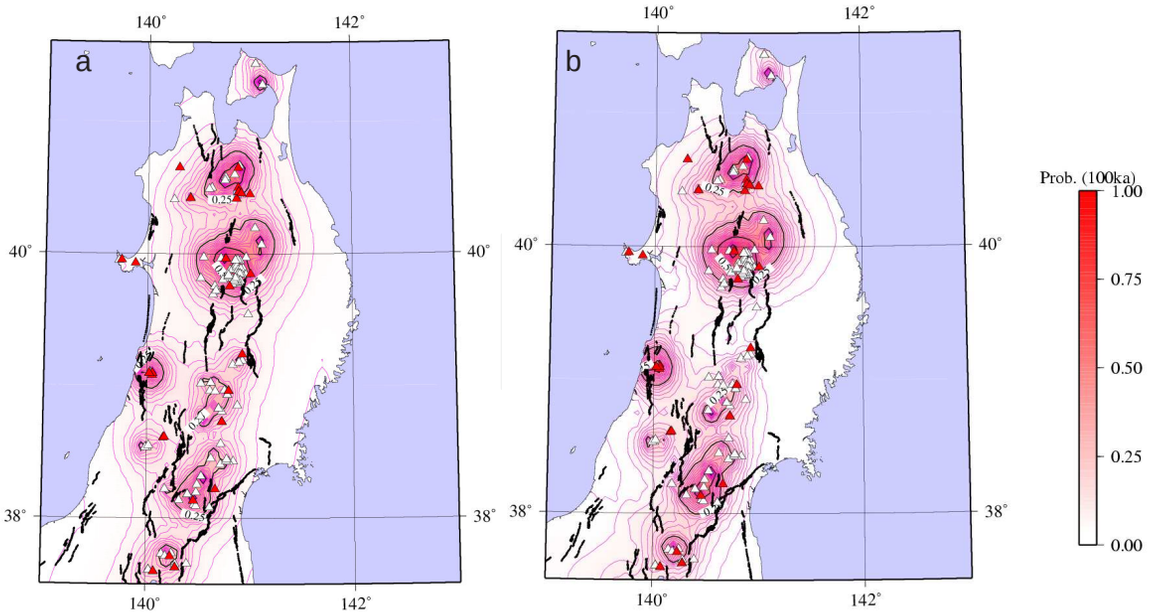

Figure 13. Verification probability plots calculated using all volcanic events before 100 ka (white triangles) in order to predict the subsequent distribution of volcanic events that formed from 100 ka to present (red triangles) for (a) the *a priori* probability (Cauchy, h=1.5km, eruption volume weighting included) and the *a posteriori* probability (b) conditioned on R/R_A ratios.

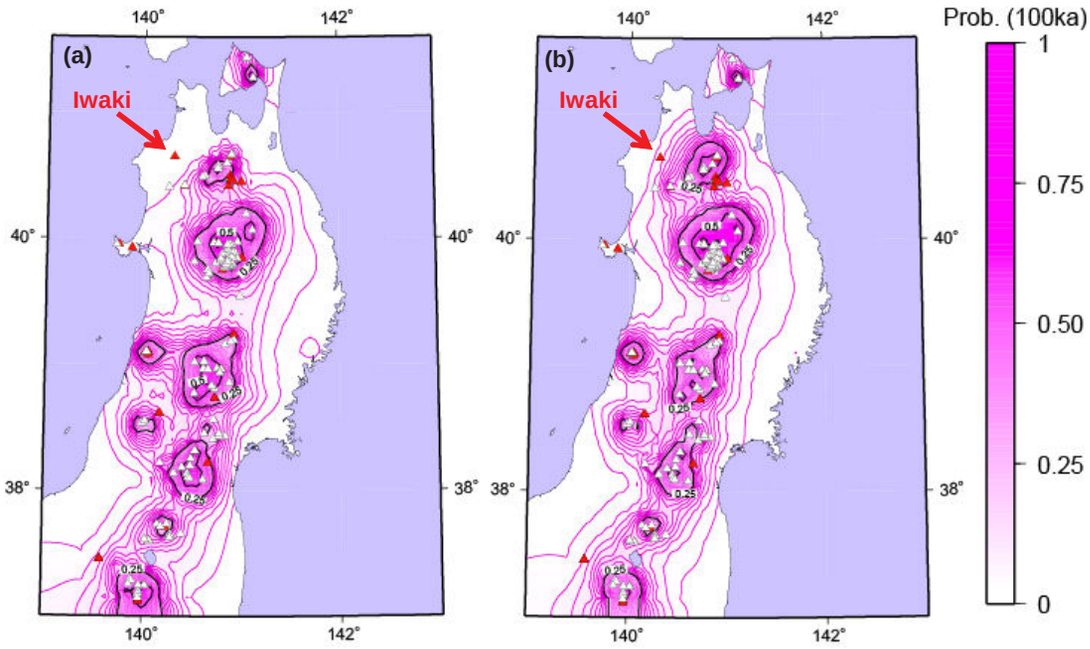

Figure 14. Verification probability plots calculated using all volcanic events before 100 ka (white triangles) in order to predict the subsequent distribution of volcanic events that formed from 100 ka to present (red triangles): (a) Cauchy kernel (h = 1.5 km) conditioned on $\Delta V / V$ at 40 km depth, (b) Cauchy kernel (h = 1.5 km) conditioned on geothermal gradient and $\Delta V / V$ at 10 and 40 km depths. (Figure modified from [1]).

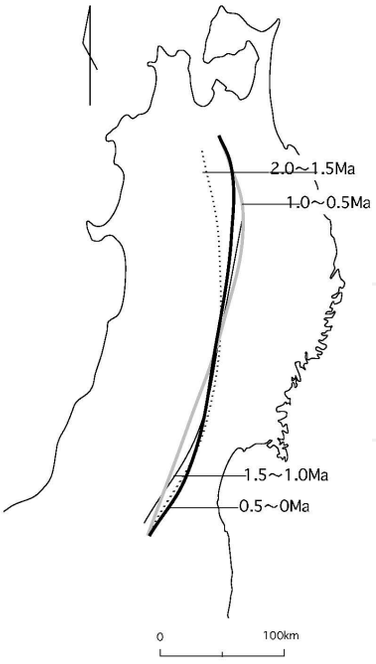

Figure 15. Shift in the volcanic front in Tohoku (compiled from [60])

care is needed. In addition to temporal recurrence rates, the type of volcanism can also change over extended timeframes. For example, [28] used eruptive volumes of volcanic products along the volcanic front in Tohoku to identify three sub-stages with distinct types of volcanism and volumetric changes in the last 2.0 Ma. From 2.0 to 1.2 Ma large-scale felsic eruptions were predominant; during 1.2 to 0.5 Ma, the crustal stress changed to compression yielding the formation of strato-volcanoes all along the Tohoku volcanic arc. Finally, from 0.5 Ma to the present day, volcanically active areas became localized [34]. The volcanic front also shifted over a 2.0 Ma period [60] (Figure 15)

It can thus be argued that for periods beyond 0.1Ma, it is unreasonable to treat $\lambda_t$in equation (3) as constant or steady state. One option might be to assign say a Weibull function where recurrence rates can increase or decrease with time [61] if there is sufficient age data to indicate temporal trends statistically. Alternatively one could assume that the temporal recurrence rates are entirely random with a tendency to cluster temporally [e.g. 22, 62]. Moreover, [22] showed that time clustering can have an impact on the spatial intensity of volcanoes.

A challenge though with utilizing temporal data are the quantity and quality of the age datasets and being consistent enough with the temporal definitions since eruptions may last for several days, weeks, months, years even longer. Having a consistent temporal definition is especially challenging when handling volcanic datasets on the regional scale described in this chapter. As highlighted in section 3, even for monogenetic volcanoes, the temporal definition is not so straightforward [41]. It was for this reason [42] argued that a drawback with nearest-neighbour models which are a function of both spatial and temporal parameters is that they require the ages of every single volcanic event within the volcanic field in question. Nevertheless in certain

http://dx.doi.org/10.5772/51859

cases such as tectonically controlled basaltic fields, eruptions can be time predictable, [63] hence there is potential to improve on the Bayesian model presented here by taking into account time clustering in the temporal rate parameter.

6. Conclusions

Bayes' thereom is a powerful statistical tool for incorporating additional datasets. In this chapter R/R_A ratios were used in probabilistic volcanic hazard assessments applying the methodology developed by [1]. These were compared with earlier assessments in Tohoku incorporating low P perturbations at 10km and 40km depth and geothermal gradients. Probabilities of one or more volcanic event(s) forming in Tohoku for both analyses were found to be similar ranging from 10^{-10} – 10^{-9} /a between clusters and 10^{-5} /a within clusters. The Cauchy kernel, combined with multiple datasets successfully captures all subsequent volcanic events, including extreme events. This is particularly important when making calculations over 1Ma when the tectonic setting is likely to change resulting in a potential shift of the volcanic front. Although the Cauchy kernel appears to be over conservative for regions east of the volcanic front, where probabilities are expected to be negligible, values are reduced when R/R_A ratios are included.

Acknowledgements

Diagrams of the probability plots were made using Generic Mapping Tools (GMT) [64]. The authors thank the constructive comments made by two anonymous reviewers which improved the manuscript.

Author details

Andrew James Martin[1], Koji Umeda[2] and Tsuneari Ishimaru[2]

1 National Cooperative for the Disposal of Radioactive Waste (NAGRA), Wettingen, Switzerland

2 Japan Atomic Energy Agency (JAEA), Toki, Japan

References

[1] Martin, A. J., Umeda, K., Connor, C. B., Weller, J. N., Zhao, D. and Takahashi, M. (2004), Modeling long-term volcanic hazards through Bayesian inference: An exam-

ple from the Tohoku volcanic arc, Japan. *J. Geophys. Res., 109,* B10208, doi: 10.1029/2004JB003201.

[2] Wickman, F. E. (1966), Repose period patterns of volcanoes, *Ark. Mineral. Geol., 4,* 291-301.

[3] Wadge, G. (1982), Steady state volcanism: Evidence from eruption histories of polygenetic volcanoes, *J. Geophys. Res. 87,* 4035-4049.

[4] Klein, F. W. (1984), Eruption forecasting at Kilauea Volcano, Hawaii, *J. Geophys. Res., 89,* 3059-3073.

[5] Sornette, A., J. Dubois, J. L. Cheminee, and D. Sornette (1991), Are sequences of volcanic eruptions deterministically chaotic? *J. Geophys. Res., 96,* 11,931-11,945.

[6] Dubois, J., and J. L. Cheminee (1991), Fractal analysis of eruptive activity of some basaltic volcanoes, *J. Volcanol. Geotherm. Res., 45,* 197-208.

[7] Pyle, D. M. (1998), Forecasting sizes and repose times of future extreme volcanic events, *Geology, 26,* 367-370.

[8] Wadge, G., P. A. V. Young, and I. J. McKendrick (1994), Mapping lava flow hazards using computer simulation. *J. Geophys. Res. 99,* 489-504.

[9] Connor L. J., C. B. Connor, K. Meliksetian and I. Savov (2012). Probabistic approach to modeling lava flow inundation: a lava flow hazard assessment for a nuclear facility in Armenia. *J. App. Volc. 1*, 3-19.

[10] Crowe, B. M., M. E. Johnson, and R. J. Beckman (1982), Calculation of the probability of volcanic disruption of a high-level radioactive waste repository within southern Nevada, USA. *Radioact. Waste Manage. Nucl, Fuel Cycle, 3,* 167-190.

[11] International Atomic Energy Agency (1997), Volcanoes and associated topics in relation to nuclear power plant siting, a safety guide, *Provisional Safety Stand. Ser.* 1, 49 pp., Vienna, Austria.

[12] Weller, J. N., A. J. Martin, C. B. Connor, and L. Connor (2006), Modelling the spatial distribution of volcanoes: An example from Armenia, in *Statistics in Volcanology*, edited by Mader, H. M., Coles, S. G., Connor, C. B. and Connor, L. J, pp. 296, Geol. Soc. Lon. on behalf of IAVCEI.

[13] McBirney, A., L. Serva, M. Guerra and C. B. Connor (2003), Volcanic and seismic hazards at a proposed nuclear power site in central Java, *J. Volcanol. Geotherm. Res., 126,* 11-30.

[14] Woods A. W., Sparks S., Bokhove, O., LeJeune A. M., Connor C. B. and Hill B. E. (2002), Modeling magma-drift interaction at the proposed high-level radioactive waste repository at Yucca Mountain, Nevada, USA. Geophys. Res. Lett. 29 (13), 1641, doi:10.1029/2002GL014665

http://dx.doi.org/10.5772/51859

[15] Connor, C. B., J. A. Stamatakos, D. A. Ferrill, B. E. Hill, I. Goodluck,, F. Ofoegbu, M. Conway, S. Budhi, and J. Trapp (2000), Geologic factors controlling patterns of small-volume basaltic volcanism: Application to a volcanic hazards assessment at Yucca Mountain, Nevada, *J. Geophys. Res., 105,* 417-432.

[16] Selva J., Orsi G., Di Vito M. A., Marzocchi W., Sandri L. (2012) Probability hazard map for future vent opening at the Campi Flegrei caldera, Italy. *Bull. Volc.* 74: 497-510

[17] Ozima, M., and F. A. Podosek (2002), *Noble Gas Geochemistry*, 2nd ed., 286 pp., Cambridge Univ. Press, New York.

[18] Hilton, D. R. (2007), Geochemistry - The leaking mantle, *Science, 318,* 1389-1390.

[19] Sano, Y., and H. Wakita, (1985), Geographical distribution of $^{3}He/^{4}He$ ratios in Japan: Implications for arc tectonics and incipient magmatism, *J. Geophys. Res., 90,* 8729-8741.

[20] Umeda, K., K. Asamori, A. Ninomiya, S. Kanazawa, and T. Oikawa (2007), Multiple lines of evidence for crustal magma storage beneath the Mesozoic crystalline Iide Mountains, northeast Japan. *J. Geophys. Res., 112,* B05207, doi:10.1029/2006JB004590.

[21] Marti J., and Felpeto A. (2010), Methodology for the computation of volcanic susceptibility An example for mafic and felsic eruptions on Tenerife (Canary Islands). *J. Volcanol. Geotherm. Res.,* 195, 69-77.

[22] Jaquet, O, C. Lantuejoul, and J. Goto (2012), Probabilistic estimation of long-term volcanic hazard with assimilation of geophysics and tectonic data. *J. Volcanol. Geotherm. Res.* 235-236: 29-36, doi:10.1016/j.jvolgeores.2012.05.003.

[23] Hasegawa, A., N. Umino, and A. Takagi (1978), Double-planed structure of the deep seismic zone in the northeastern Japan arc, *Tectonophysics, 47,* 43-58.

[24] Nakagawa, M., H. Shimotori, and T. Yoshida (1986), Aoso-Osore volcanic zone- The volcanic front of the northeast Honshu arc, Japan, *Journal of the Japan Association of Mineralogy and Economic Geology, 81,* 471-478.

[25] Hasegawa, A., S. Horiuchi, and N. Umino (1994), Seismic structure of the northeastern Japan convergent margin: A synthesis, *J. Geophys. Res., 99,* 22,295-22,311.

[26] Yoshida, T., T. Oguchi, and T. Abe (1995), Structure and evolution of source area of the Cenozoic volcanic rocks in Northeast Honshu arc, Japan, *Memoirs of the Geological Society of Japan, 44,* 263-308.

[27] Takahashi, M. (1995), Large-volume felsic volcanism and crustal strain rate, *Bulletin of the Volcanological Society of Japan, 40,* 33-42.

[28] Umeda, K., S. Hayashi, M. Ban, M. Sasaki, T. Oba, and K. Akaishi (1999), Sequence of volcanism and tectonics during the last 2.0 million years along the volcanic front in Tohoku district, NE Japan, *Bulletin of the Volcanological Society of Japan, 44,* 233-249.

[29] Zhao, D., F. Ochi, A. Hasegawa, and A. Yamamoto (2000), Evidence for the location and cause of large crustal earthquakes in Japan, *J. Geophys. Res., 105,* 13,579-13,594.

[30] Committee for Catalog of Quaternary Volcanoes in Japan (1999), eds. Catalog of Quaternary volcanoes in Japan [CD-ROM], *The Volcanological Society of Japan*.

[31] Hayakawa, Y. (1985), Pyroclastic geology of Towada volcano, *Bulletin of the Earthquake Research Institute, University of Tokyo*, *60,* 507-592.

[32] Ban, M., S. Hayashi and N. Takaoka, K-Ar dating of the Chokai volcano, northeast Japan arc: A compound volcano composed of continuously established three stratovolcanoes, 46, 317 – 333.

[33] Oki, J., N. Watanabe, K. Shuto, and T. Itaya (1993), Shifting of the volcanic fronts during Early to Late Miocene age in the Northeast Japan arc, *The Island Arc, 2,* 87-93.

[34] Kondo, H., K. Kaneko, and K. Tanaka (1998), Characterization of spatial and temporal distribution of volcanoes since 14 Ma in the northeast Japan arc, *Bulletin of the Volcanological Society of Japan, 43,* 173-180.

[35] Koyama, M., Y. Hayakawa, and F. Arai (1995), Eruptive history of the Higashi-Izu Monogenetic Volcano field 2: Mainly on volcanoes older than 32,000 years ago, *Kazan*, *40,* 191-209.

[36] Sheridan, M. F. (1992), A Monte Carlo technique to estimate the probability of volcanic dikes, paper presented at Third International Conference on High-Level Radioactive Waste Management, Am. Nucl. Soc., La Grange Park, Ill., 2033-2038.

[37] Lutz, T. M., and J. T. Gutmann (1995), An improved method for determining and characterizing alignments of point like features and its implications for the Pinacate volcanic field, Sonora, Mexico, *J. Geophys. Res. 100,* 17,659-17,670.

[38] Condit, C. D., and C. B. Connor (1996), Recurrence rates of volcanism in basaltic volcanic fields: An example from the Springerville volcanic field, Arizona, *Geol. Soc. Am. Bull., 108,* 1225-1241.

[39] Kienle J., P. R. Kyle, S. Self, R. J. Motyka and V. Lorenz, (1980), Ukinrek Maars, Alaska: I, April 1977 eruption sequence, petrology and tectonic setting: *J. Volcanol. Geotherm. Res., 7*, 11-37.

[40] Nemeth K. and S. J. Cronin (2011), Drivers of explosivity and elevated hazard in basaltic fissure eruptions: The 1913 eruption of Ambrym Volcano, Vanuatu (SW-Pacific). *Jour. Volcanol. Geoth. Res., 201,* 194-209, doi: 10.1016/j.jvolgeores.2010.12.007.

[41] Kereszturi, G., K. Nemeth, G. Csillag, K. Balogh and J. Kovacs (2011). The role of external environmental factors in changing eruption styles of monogenetic volcanoes in a Mio/Pleistocene continental volcanic field in western Hungary *J. Volcanol. Geotherm. Res.,* 201, 227-240. doi: 10.1016/j.jvolgeores.2010.08.018.

http://dx.doi.org/10.5772/51859

[42] Connor, C. B., and B. E. Hill (1995), Three nonhomogenous Poission models for the probability of basaltic volcanism: Application to the Yucca Mountain region, Nevada. *J. Geophys. Res., 100,* 10,107-10,125.

[43] Martin, A. J., M. Takahashi, K. Umeda, and Y. Yusa (2003), Probabilistic methods for estimating the long-term spatial characteristics of monogenetic volcanoes in Japan, *Acta. Geophys., Pol.,51,* 271-291.

[44] Takahashi, M. (1994), Structure of polygenetic volcano and its relation to crustal stress field: 1. Stable and unstable vent types, *Bulletin of the Volcanological Society of Japan, 39,* 191-206.

[45] Tarantola, A. (1990), Probabilistic Foundations of Inverse Theory, in *Oceanographic and Geophysical Tomography*, edited by Y. Desaubies, A. Tarantola and J. Zinn-Justin, pp. 1-27, Elsivier Science Publishers B. V.

[46] Debski, W. (2004), Application of Monte Carlo techniques for solving selected seismological inverse problems, *Publications of the Institute of Geophysics, Polish Academy of Sciences, B-34 (367)*, 207 pp., Warszawa, Poland.

[47] Gelman, A., J. B. Carlin, H. S. Stern, and D. B. Rubin (1995), *Bayesian Data Analysis*, 526 pp., Chapman and Hall/CRC, Boca Raton.

[48] de Bremond d'Ars, J., C. Jaupart, and R. S. J. Sparks (1995), Distribution of volcanoes in active margins, *J. Geophys. Res., 100,* 20,421-20,432.

[49] Cressie, N. A. C. (1991), *Statistics for Spatial Data*, 900 pp., John Wiley, New York.

[50] Hayashi, S., K. Umeda, M. Ban, M. Sasaki, M. Yamamoto, T. Oba, K. Akaishi, and T. Oguchi (1996), Temporal and spatial distribution of Quaternary volcanoes in northeastern Japan (1) - Spreading of volcanic area toward back-arc side – *Program and Abstract, Volcanological Society of Japan,* no. 2, 71-71.

[51] Clark, P. J., and F. C. Evans (1954), Distance to nearest neighbour as a measure of spatial relationships in populations. *Ecology, 35,* 445-453.

[52] Diggle, P. J. (1985), A kernel method for smoothing point process data, *Appl. Statist., 34,* 138-147.

[53] AIST (2009), Active fault database of Japan, version 2009. Research Information Database DB095, National Institute of Advanced Industrial Science and Technology. http://riodb02.ibase.aist.go.jp/activefault/index_e.html

[54] Wakita, H., and Y. Sano (1983), $^{3}He/^{4}He$ ratios in CH_4-rich natural gases suggest magmatic origin, *Nature, 305*, 792-794.

[55] Sano, Y., Y. Nakamura, and H. Wakita (1985), Areal distribution of $^{3}He/^{4}He$ ratios in the Tohoku district, Northeastern Japan, *Chem. Geol., 52*, 1-8.

[56] Nakajima, J., T. Matsuzawa, A. Hasegawa and D. Zhao (2001), Three-dimensional structure of Vp, Vs and Vp/Vs beneath northeastern Japan: Implications for arc magmatism and fluids, J. Geophys. Res., 106, 21,843 – 21,857, doi:10.1029/2000JB000008

[57] Tamanyu S., K. Sakaguchi, T. Sato and M. Kato (2008), Integration of geological and geophysical data for extraction of subsurface thermal and hydrothermal anomaly areas – Examples in Tohoku and Chugoku/Shikoku districts, Japan, *Bulletin of the Geological Survey of Japan, 59,* 7-26.

[58] Zhao, D., A. Hasegawa, and S. Horiuchi (1992), Tomographic imaging of P and S wave velocity structure beneath northeastern Japan, *J. Geophys. Res., 97,* 19,909-19,928.

[59] Zhao, D. (2001), Seismological structure of subduction zones and its implications for arc magmatism and dynamics, *Phys. Earth Planet. Int., 127,* 197-214.

[60] Umeda. K., H. Osawa, T. Nohara, E. Sasao, O. Fujiwara, K. Asamori, and N. Nakatsuka (2005), Current status of the geoscientific research for long-term stability of the geological environment in JNC's R& D programme, *Journal of Nuclear Fuel Cycle and Environment,* 11, 97-112.

[61] Ho, C-H. (1991), Nonhomogenous Poisson model for volcanic eruptions, *Mathematical Geology, 23,* 167-173.

[62] Jaquet, O., S. Low, B. Martinelli, V. Dietrich, and D. Gilby (2000), Estimation of volcanic hazards based on Cox stochastic processes, *Physics and Chemistry of the Earth, Part A: Solid Earth and Geodesy, 25*, 571-579.

[63] Valentine, G. A. and F. Perry (2007). Tectonically controlled, time-predictable basaltic volcanism from a lithospheric mantle source (central Basin and Range Province, USA). Earth Planet. Sci. Lett., 261, 201-216, doi: 10.1016/j.epsl.2007.06.029.

[64] Wessel, G. P. L., and W. H. F. Smith (1998), New improved version of the generic mapping tools released, *Eos, 79*, 579.